Cellulose nanofibril formulations incorporating a low molecular weight alginate oligosaccharide modify bacterial biofilm development

Alison A. Jack, [†] Henriette R. Nordli,[‡] Lydia C. Powell,[†] Damian J. J. Farnell,[†] Brita Pukstad,[‡,‖] Philip D. Rye,[⊥] David W. Thomas[†], Gary Chinga-Carrasco*[,§], Katja E. Hill*[,†]

[†]Advanced Therapies Group, Oral and Biomedical Sciences, Cardiff University School of Dentistry, Cardiff, CF14 4XY, UK

[‡]Department of Cancer Research and Molecular Medicine, NTNU, Trondheim, Norway

[§]RISE PFI, Høgskoleringen 6b, NO-7491 Trondheim, Norway

[‖]Department of Dermatology, St. Olavs Hospital, Trondheim University Hospital, Trondheim, Norway

[⊥]AlgiPharma AS, Sandvika, Norway

Corresponding authors.
*E-mail: hillke1@cardiff.ac.uk (K. Hill)
*E-mail: gary.chinga.carrasco@rise-pfi.no (G. Chinga-Carrasco)

Keywords: Nanocellulose, Biofilms, *Pseudomonas aeruginosa*, *Staphylococcus aureus*, COMSTAT image analysis, OligoG

ABSTRACT

Cellulose nanofibrils (CNFs) from wood pulp are a renewable material possessing advantages for biomedical applications, due to their customizable porosity, mechanical strength, translucency and environmental biodegradability. Here we investigated the growth of multi-species wound biofilms on CNF formulated as aerogels and films incorporating the low molecular weight alginate oligosaccharide OligoG CF-5/20 to evaluate their structural and antimicrobial properties. Overnight microbial cultures were adjusted to 2.8 x 10^9 colony forming units (cfu) mL^{-1} in Mueller Hinton broth and growth rates of *P. aeruginosa* PAO1 and *S. aureus* 1061A monitored for 24 h in CNF dispersions sterilized by γ-irradiation. Two CNF formulations were prepared (20 g m^{-2}) with CNF as air-dried films or freeze-dried aerogels, with or without incorporation of an antimicrobial alginate oligosaccharide (OligoG CF-5/20) as a surface coating or bionanocomposite respectively. The materials were structurally characterized by scanning electron microscopy (SEM) and laser profilometry (LP). The antimicrobial properties of the formulations were assessed using single- and mixed-species biofilms grown on the materials and analysed using LIVE/DEAD® staining with confocal laser scanning microscopy (CLSM) and COMSTAT software. OligoG-CNF suspensions significantly decreased the growth of both bacterial strains at OligoG concentrations >2.58% ($P<0.05$). SEM showed that aerogel-OligoG bionanocomposite formulations had a more open 3-dimensional structure, while LP showed film formulations coated with OligoG were significantly smoother than untreated films or films incorporating PEG400 as a plasticizer ($P<0.05$). CLSM of biofilms grown on films incorporating OligoG demonstrated altered biofilm architecture, with reduced biomass and decreased cell-viability. The OligoG-CNF formulations as aerogels or films both inhibited pyocyanin production ($P<0.05$). These novel CNF formulations or bio-nanocomposites were able to modify bacterial growth, biofilm development and virulence factor production *in vitro.* These data support the potential of OligoG and CNF bio-nanocomposites for use in biomedical applications where prevention of infection or biofilm growth is required.

INTRODUCTION

In the last 10 years, nanocellulose research has expanded exponentially. Nanocellulose includes cellulose nanofibrils (CNFs), cellulose nanocrystals (CNCs) and bacterial cellulose (BC). As a potentially inexhaustible natural polymer from sustainable sources, its bio-sustainability is a major driving force behind this increased interest.[1] Nanocelluloses possess a myriad of useful material properties such as biodegradability in nature, mechanical strength, modifiable surface chemistry and biocompatibility which may be applied in a wide range of industrial and clinical applications.[2] One of these applications is in the design of wound dressing materials.

Chronic, non-healing skin wounds are an important, often recognized source of morbidity,[3] which is increasing in incidence annually, with the ageing population and the inexorable rise of obesity and diabetes. In health, the skin is colonized by a diverse "reservoir" of pathogenic and beneficial bacteria, which do not abnormally affect the host. In disease however, pathogens from the normal skin microbiota can become a serious problem in terms of infection, morbidity and quality of life. Infections in chronic wounds have been found to be associated with the presence of bacterial biofilms in up to 75% of cases.[4] Bacteria in these biofilms are encased in a charged "polymeric mesh" of host- and bacteria-derived extracellular polymers which resist physical and chemical (antimicrobial) disruption and have increased resistance to antimicrobial and antibiotic therapy due to both the physical barrier, and also alterations of bacterial metabolism within the biofilm matrix.[5] Chronic wounds are polymicrobial, the most common isolates being the commensals, *Pseudomonas aeruginosa* and *Staphylococcus aureus.*[6] Whilst the aetiology of non-healing wounds is undoubtedly multi-factorial, bacteria play a significant role in perpetuating the inflammation and proteolytic wound environment. Indeed, studies have demonstrated impaired wound healing associated with bacterial and fungal colonization.[7,8]

In the current treatment of chronic wounds a wide array of wound dressings are employed varying in their physical composition (films, foams, hydrogels, hydrocolloids) and biological activity (dermis, cell-based products and anti-bacterial compounds) and are made from an increasing number of materials such as polyurethane, carboxymethylcellulose and natural polymers e.g. collagen, alginates, starches, and hyaluronic acid.[9]

The potential to "customize" nanocellulose dressing materials with different mechanical and physical properties for distinct indications in wound dressing materials

now exists. Indeed, we recently described the use of CNFs from wood pulp as a prototype wound dressing material.[10,11] Nanofibrils are produced mechanically from cellulose fibers by the use of high-pressure homogenisation and/or grinding which de-laminates the fibers, releasing the nanofibrils. The longer the homogenisation steps, the more nanofibrils are liberated.[12] The use of chemical pre-treatments, such as TEMPO-mediated oxidation,[13] may not only selectively introduce carboxylate groups onto the surface of the CNFs,[14] but also radically reduce the energy costs for the mechanical processing; making the homogenisation steps more cost-effective.[15] Hence, a combination of chemical and mechanical treatments are often used. Above a critical concentration, TEMPO nanofibrils display gel-like properties in water[16] and have a high aspect ratio, lengths in the micrometre-scale and widths of ~4 nm.[17]

The abundance of CNFs from renewable sources, its relatively low cost, its natural biodegradability and its excellent mechanical properties are all distinct advantages for its exploitation as a wound dressing material. Moreover, its ability to "self-assemble" into 3-dimensional micro-porous structures confers a high capacity for absorbance; a useful property in wounds with high levels of wound exudate.[18] The ability to now produce wood CNF that is ultrapure (low endotoxin), with low cytotoxicity levels, also reinforces its potential as a material for biomedical applications, such as "scaffolds" in wound dressings.[19] Manipulation and tailoring of the CNF hydrophilic surface chemistry can be used to functionalize the materials to make them pH responsive or to allow incorporation of antimicrobial agents. We previously demonstrated that the physical form of CNF-derived materials may vary dependent upon their formulation; being antimicrobial in suspension as hydrogels (against *P. aeruginosa*) but not when prepared as films or aerogels.[11] We have also established how porosity and surface roughness may influence bacterial growth on the CNF aerogels, with less biofilm growth being associated with lower porosity and roughness. For wound dressing materials, the design of CNF materials with intrinsic antibacterial ability would clearly be useful.

OligoG is a natural product derived from alginate extracted from the stem of the brown seaweed *Laminaria hyperborea*, and possesses antibacterial[20-25] and antifungal properties.[26,27] Unlike antibiotics and silver, prolonged exposure to OligoG does not lead to the acquisition of resistance.[20] These antimicrobial properties, combined with the excellent safety profile, make alginate oligosaccharides potentially useful for incorporation into dressing materials for use in wound healing.

To further investigate the potential clinical application of CNF dressing materials in chronic human skin wound healing, we examined single and mixed species biofilms grown on CNF prepared as two different structural formulations (aerogels and films) with or without incorporation of the antimicrobial OligoG.

MATERIALS AND METHODS

CNF Production. *Pinus radiata* bleached kraft pulp fibers were used as the raw material for CNF production. The pulp fibers were pretreated with TEMPO-mediated oxidation[28] using 3.8 mM hypochlorite (NaOCl) g^{-1} cellulose. The pre-treated fibers were then extensively washed with deionized water until the conductivity was below 5 µS/cm. The CNF were produced through homogenization using a Rannie 15 type 12.56X homogenizer. The material (1% solids content) was homogenized with a pressure drop of 1000 pascal units and collected after 2 or 3 passes through the homogenizer.

Sample Preparation. CNF samples (Table 1) were produced by solution casting in sterile petri dishes, followed by either air-drying to produce low porosity films or freeze-drying to yield more porous aerogel structures. PEG400 was incorporated into the films for increased plasticity[29] with 40% PEG shown to be sufficient to improve the ductility of the films, whilst having adequate liquid absorption and without affecting its' cytocompatibility. In addition, the antimicrobial OligoG derived from marine algae[20] was either incorporated into the CNF aerogels to produce a bionanocomposite or surface-coated onto the CNF films.

CNF materials (for the dried films and aerogels) were used as 0.2% suspensions (grammage 20 g m^{-2}) throughout. Bionanocomposite films were made using 0.2% (w/v) twice homogenised CNF dispersions ±PEG400 (40%, w/v) which were air-dried at room temperature (~20°C) for 5-7 days. Surface coating with OligoG was performed on air-dried films using a 0.2% (w/v) OligoG solution, by pouring this evenly onto the film surface within the petri-dish and allowing it to air-dry at 37°C for 48 h to a final concentration of 0.9 mg cm^{-2} film (as determined by weight of material before and after coating). Freeze-dried aerogels were prepared using 0.2% (w/v) thrice homogenised CNF dispersions ± OligoG (to give a final concentration of 2%), before being frozen in petri dishes at -20ºC and freeze-dried for 48 h.

All the samples were cut into 1 or 2 cm^2 sections and sterilized by γ-irradiation (15 kGy). Commercially-available wound dressings AquaCel® and AquaCel Ag® (ConvaTec Ltd, Deeside) were used as controls.

Table 1. Characteristics and Absorbency (n=3) of the CNF Materials Used.

CNF material	Sample name	No. of homogenisation steps used[10,11]	OligoG concentration (%)	PEG400 (%)	Fluid Absorption (g/g)
Aerogel	A0.2	3	0	0	111.65
Aerogel	A0.2G	3	2‡	0	11.31
Film	F0.2	2	0	0	5.83
Film	F0.2G	2	0.2§	0	8.11
Film	F0.2P†	2	0	40‡	6.70
Control	AquaCel®				25.46[11]
Control	AquaCel Ag®				26.28[11]

†PEG400 incorporated into the film to enhance plasticity.
‡Bio-nanocomposite, with 2% OligoG CF-5/20 incorporated into the aerogels.
§OligoG CF-5/20 (0.2%) surface coating of films to a final concentration of 0.9 mg cm^{-2}.

Absorption Measurements. Fluid absorption of the test and control materials was assessed as previously described.[11]

Screening for the Ability of CNF to Support Bacterial Growth. Jack et al. (2017) originally examined the growth of *P. aeruginosa* in CNF hydrogels. For this study, the ability of the same CNF dispersions (homogenised three times) to inhibit or promote growth of another wound bacterium, *S. aureus*, in planktonic culture was also examined. CNF dispersions were prepared at 0.2, 0.4 or 0.6% (w/v) and sterilized by γ-irradiation.

For the growth curves, overnight bacterial cultures of *P. aeruginosa* PAO1 and *S. aureus* 1061A (both wound isolates) were diluted to 2.8 x 10^9 cfu mL^{-1} in either Mueller-Hinton (MH) broth, PBS or deionized water, and mixed 1:2 (v/v) with 0.2% (w/v) CNF dispersions or water in a 24 well plate. Plates were incubated at 37°C

aerobically for 24 h measuring optical density every hour at 600 nm (OD_{600}) in a FLUOstar Optima plate reader (BMG LABTECH).

Log_{10} reduction assay. Time-kill assays were used to evaluate the antimicrobial efficacy of the aerogel and film materials against *S. aureus* 1061A in comparison to a commercially available wound dressing containing silver AquaCel (Ag)® as previously described (Jack et al 2017).

The effect of PEG400 and/or OligoG with CNF dispersions on bacterial growth. The effect of CNF dispersions with/without PEG 400 and/or OligoG on the growth of either *P. aeruginosa* PAO1 or *S. aureus* 1061A was determined using growth curves. CNF dispersions were diluted in deionized sterilized water to final concentrations of 0.2% ±OligoG CF-5/20 (0.2, 2 or 2.58%) and/or ±PEG400 (40%). Growth curves were carried out as described above.

Scanning Electron Microscopy (SEM). CNF aerogel samples (A0.2 and A0.2G) were prepared for SEM analyses by immersion in glutaraldehyde (2.5%) for 24 h, before being washed with deionised water (x4) and immersed in fresh deionised water. The samples were then frozen (24 h) and freeze-dried for 24 h. The material surface was then imaged on the Tescan Vega SEM at 5 kV.

Biofilm growth on CNF formulations. Samples (1 cm^2) of formulations A0.2 and A0.2G (aerogels) and F0.2, F0.2G and F0.2P (films) were added to a 12-well plate containing MH broth (3 mL) and 60 µL of *P. aeruginosa* PAO1 and/or *S. aureus* 1061A overnight cultures (adjusted to 6.1 x 10^9 cfu mL^{-1}). Plates were incubated at 37ºC in a static aerobic environment for 24 h before removing the supernatant and then washing the biofilms once with PBS.

Confocal Laser Scanning Microscopy (CLSM) imaging of Biofilm Growth on CNF Materials. Biofilms were stained with LIVE/DEAD® BacLight™ bacterial viability kit (Invitrogen, Paisley, UK) containing SYTO 9 dye (staining LIVE cells, green) and propidium iodide (staining DEAD cells, red) and incubated in the dark (10 min). The samples were then mounted onto microscope slides with spacers with the addition of Vectorshield (Vector Laboratories, UK), before being covered with a coverslip and sealed with clear nail-varnish. Biofilms were imaged with a Leica TCS SP5 confocal system using a x63 lens. Bacterial growth was quantified using COMSTAT image-analysis software.[30]

Effect of CNFs on Pyocyanin Production. Overnight cultures of *P. aeruginosa* PAO1 were adjusted to 6 x 10^{11} cfu mL^{-1}, and 60 µL added to MH-broth (6 mL) in a 6-

well plate and grown statically for 24 h ± CNF formulations (A0.2, A0.2G, F0.2, F0.2G and F0.2P) or AquaCel (Ag)® (2 x 2 cm^2). Bacterial cultures were then centrifuged (10000 *g*) for 10 min to produce a cell-free culture supernatant and used for the extraction of virulence factors.

Pyocyanin pigment was extracted from the cell-free supernatant using chloroform (3:2; v/v). Pyocyanin (in the chloroform-phase) was re-extracted with 0.2 M HCl (2:1; v/v) and the absorbance read at 540 nm.[31]

Laser Profilometry. To directly study the surface of the CNF materials, samples (10 mm x 10 mm) were cut from the dried film materials (F0.2, F0.2G and F0.2P) for surface analysis (and surface roughness measurements) using laser profilometry (LP) as previously described.[32] LP could not be performed on the aerogels due to the limitations of the laser beam/detector system in detecting the steep surface gradients associated with these materials.

Ion Milling. To directly study biofilm growth on the CNF materials, cross-sections of the A0.2 and A0.2G aerogels with *P. aeruginosa* PAO1 biofilm growth, (prepared as for SEM), were made by ion-milling using an IM4000 system and a milling time of 5 h at 2.5 kV. Images of the samples were then acquired using a Hitachi scanning electron microscope (SU3500) in secondary electron imaging, low-vacuum mode, using 3-5 kV acceleration voltage.

Statistical Analysis. SPSS (IBM Corp, New York, USA) or GraphPad Prism 3 (GraphPad software Inc, La Jolla, USA) were used to perform statistical analysis. The following tests were used including: minimum significant difference (MSD) calculated using the Tukey-Kramer method (growth curve data), ANOVAs of log or log(2-X) transformed data (to correct for normality) using Kw, Tukey-Kramer or Dunn's Multiple Comparisons Tests (COMSTAT and laser profilometry data) and Student's T-test (pyocyanin data). $P<0.05$ was considered significant.

RESULTS

Bacterial growth in CNF dispersions. As we have previously shown with *P. aeruginosa*,[11] *S. aureus* was unable to use CNF as a carbon source. CNF incubated with MH broth (**Supporting Information, Figure S1A**) showed good growth, but this was not seen in CNF incubated with water or PBS (**Supporting Information, Figure S1B and C**), suggesting any observed growth was solely due to the MH broth and not

the CNF. In addition, a slight inhibitory effect of the CNF hydrogel was observed compared to the MH control (**Supporting Information, Figure S1A**). This inhibitory effect was not seen in the Log10 reduction assay with the dried aerogel or film materials (**Supporting Information, Figure S1D**).

Growth curves for the wound microorganisms *S. aureus* (1061A) and *P. aeruginosa* PAO1 were performed with CNF dispersions with/without OligoG CF-5/20 and PEG400 (**Figure 1**). When grown with OligoG alone, a significant decrease in growth of both *S. aureus* (**Figure 1A;** MSD=0.1756) and *P. aeruginosa* PAO1 (**Figure 1B;** MSD=0.2489) was observed at 10%. PEG400 (40%) alone (without MH broth) did not appear to support the growth of either microorganism (**Figures 1C and 1D;** MSD=0.2241 and 0.1168 respectively). In contrast, low levels of bacterial growth were evident in PEG400 with the addition of MH, with similar growth levels also seen for the PEG400 + OligoG CF-5/20 growth curves, (at every concentration of OligoG tested) with only *P. aeruginosa* at 2.58% OligoG demonstrating any apparent, but slight, inhibition of growth.

Scanning Electron Microscopy of CNF formulations. Surface characterisation of the aerogels (A0.2 and A0.2G) using SEM demonstrated distinct differences between the two materials. The A0.2 formulation had an undulating surface, which appeared to be much denser than the CNF-OligoG bionanocomposite (A0.2G), which had a much rougher, more open network of fibres with fissures penetrating into the 3-dimensional structure (**Figure 2A**).

Laser profilometry of CNF film formulations. Laser profilometry of the films F0.2, F0.2G and F0.2P, (**Figures 2B and C)** showed distinct differences in the material surfaces, especially for the OligoG-surface coated formulation (F0.2G) and the bionanocomposite film incorporating PEG400 (F0.2P) which both exhibited significantly decreased surface-roughness ($P<0.05$). The OligoG coated film (F0.2G) was also much smoother than the bionanocomposite containing PEG (F0.2P).

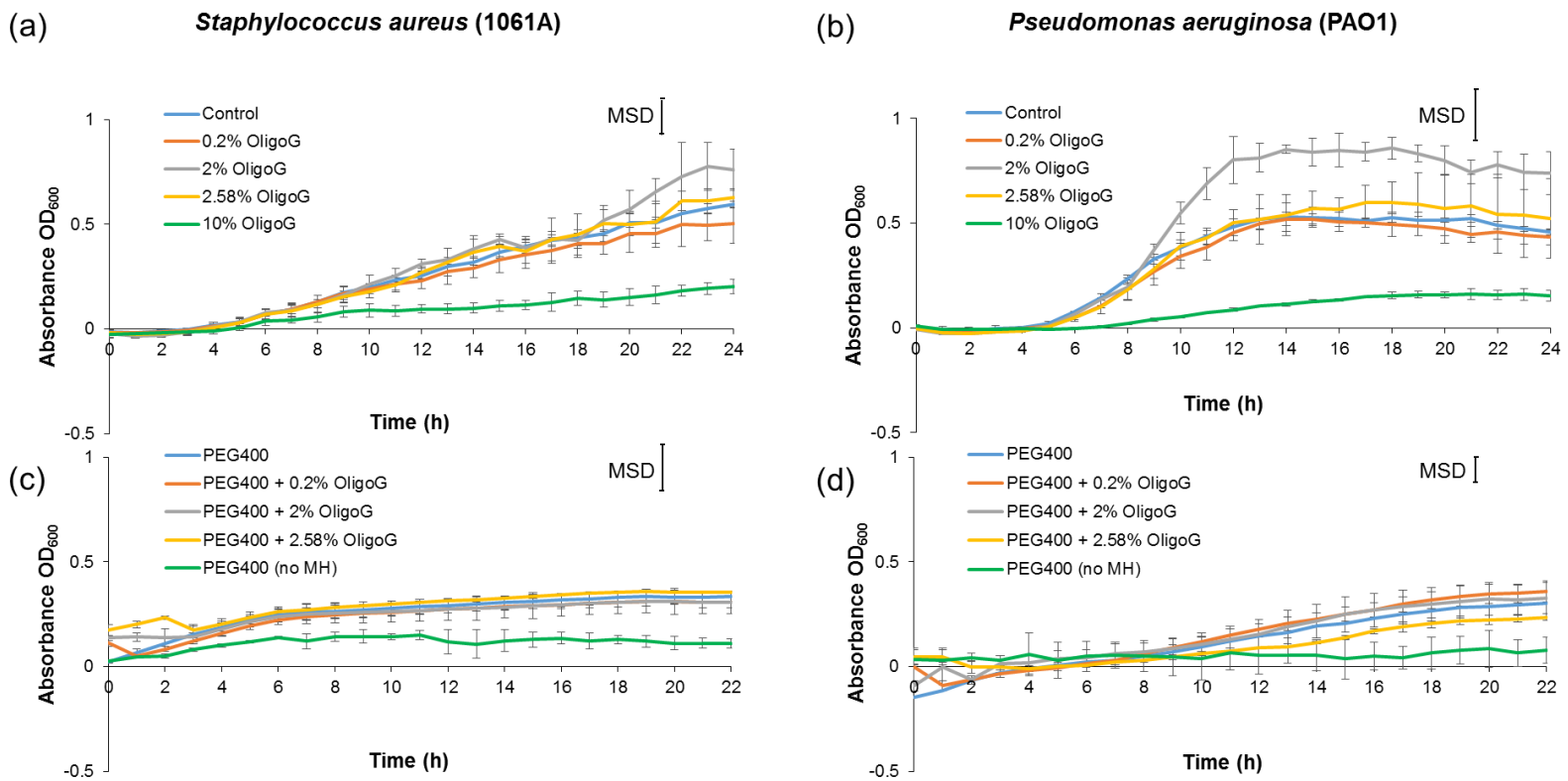

Figure 1. Effect of PEG400 (40%, w/v) and/or OligoG CF-5/20 (0.2, 2 or 2.58%) on bacterial growth in T3 CNF (0.2%) in MH broth (unless otherwise stated) of (a, c) *S. aureus* 1061A. (b, d) *P. aeruginosa* (PAO1). MSD, minimum significant difference (n=3; $P<0.05$).

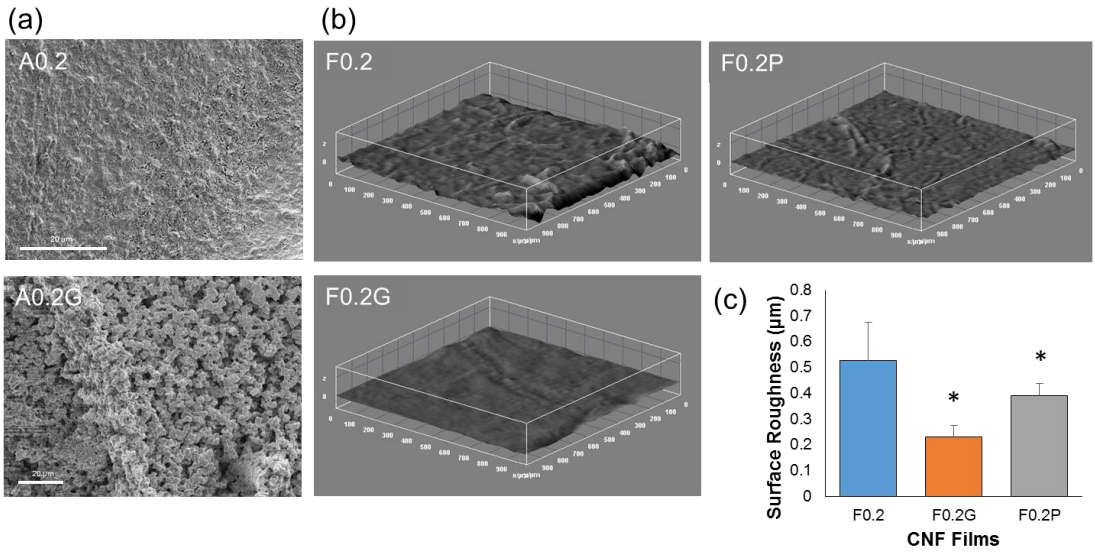

Figure 2. Structural characterization of CNF formulations. Scanning electron microscopy (SEM) of (a) aerogels A0.2 and A0.2G. (b) Laser profilometry (LP) of films F0.2, F0.2G and F0.2P. (c) Corresponding surface roughness measurements (from LP only). (*significantly different compared to the F0.2 control; n=3; P<0.05).

Confocal laser scanning microscopy of *P. aeruginosa* and *S. aureus* single and mixed species biofilms grown on CNF formulations. CLSM of biofilms grown on the films and then stained with LIVE/DEAD® cell viability dyes showed that the untreated (control) films (F0.2) produced the thickest biofilms, as well as complete surface coverage with bacteria (**Figure 3A**). for films coated with OligoG (F0.2G; **Figure 3B**), a markedly reduced bacterial biofilm biomass was evident, with significantly decreased biomass observed by Comstat analysis in both the *P. aeruginosa* and the mixed species biofilms ($p<0.05$; **Figure 3D)** which was associated with increased bacterial "clumping", i.e. aggregation, compared to that observed in the control (F0.2). However, this effect was not evident in films incorporating PEG400 (F0.2P; **Figure 3C**). In addition, significant decreases in mean thickness and significant increases in surface roughness (**Figure S2**) in single species *P. aeruginosa* and *S. aureus* biofilms were evident after growth on OligoG coated surfaces ($p<0.05$). In contrast, although mixed species biofilms grown on the CNF films with PEG400 exhibited an increased loss of cell viability when compared to *P. aeruginosa* and *S. aureus* only biofilms (**Figure 3C**), this was not shown to be significant in the Comstat analysis (**Figures 3D and S2A,B**).

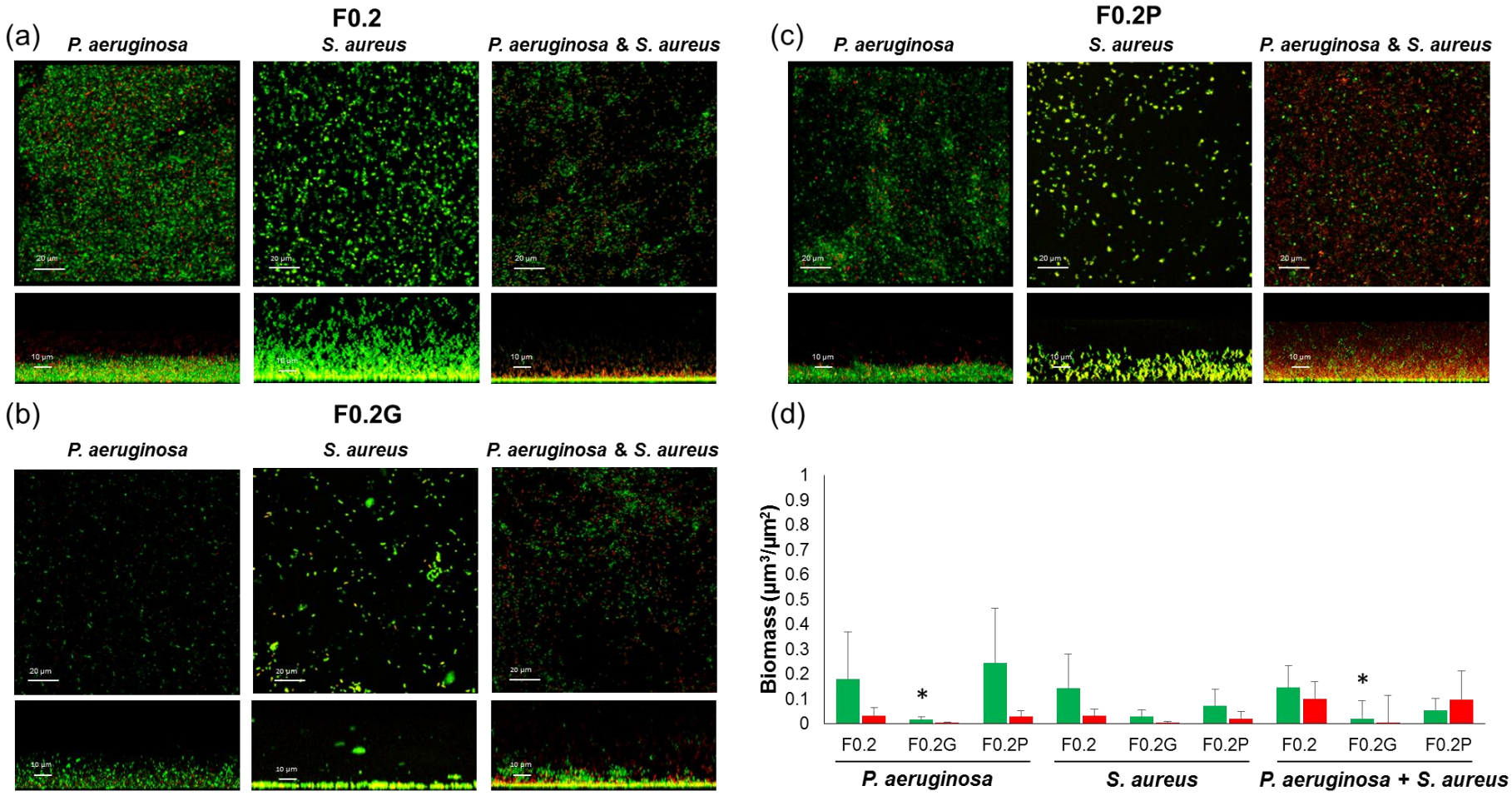

Figure 3. CLSM images of LIVE/DEAD® staining of 24 h single and dual species biofilms grown on CNF films. (a) Control F0.2. (b) OligoG-coated F0.2G. (c) PEG400 biocomposite F0.2P. COMSTAT image analysis showing (d) mean biofilm biomass of LIVE (green) and DEAD (red) cells. (*significantly different compared to the equivalent no OligoG control; n=10 images each from n=3 replicates; $P<0.05$).

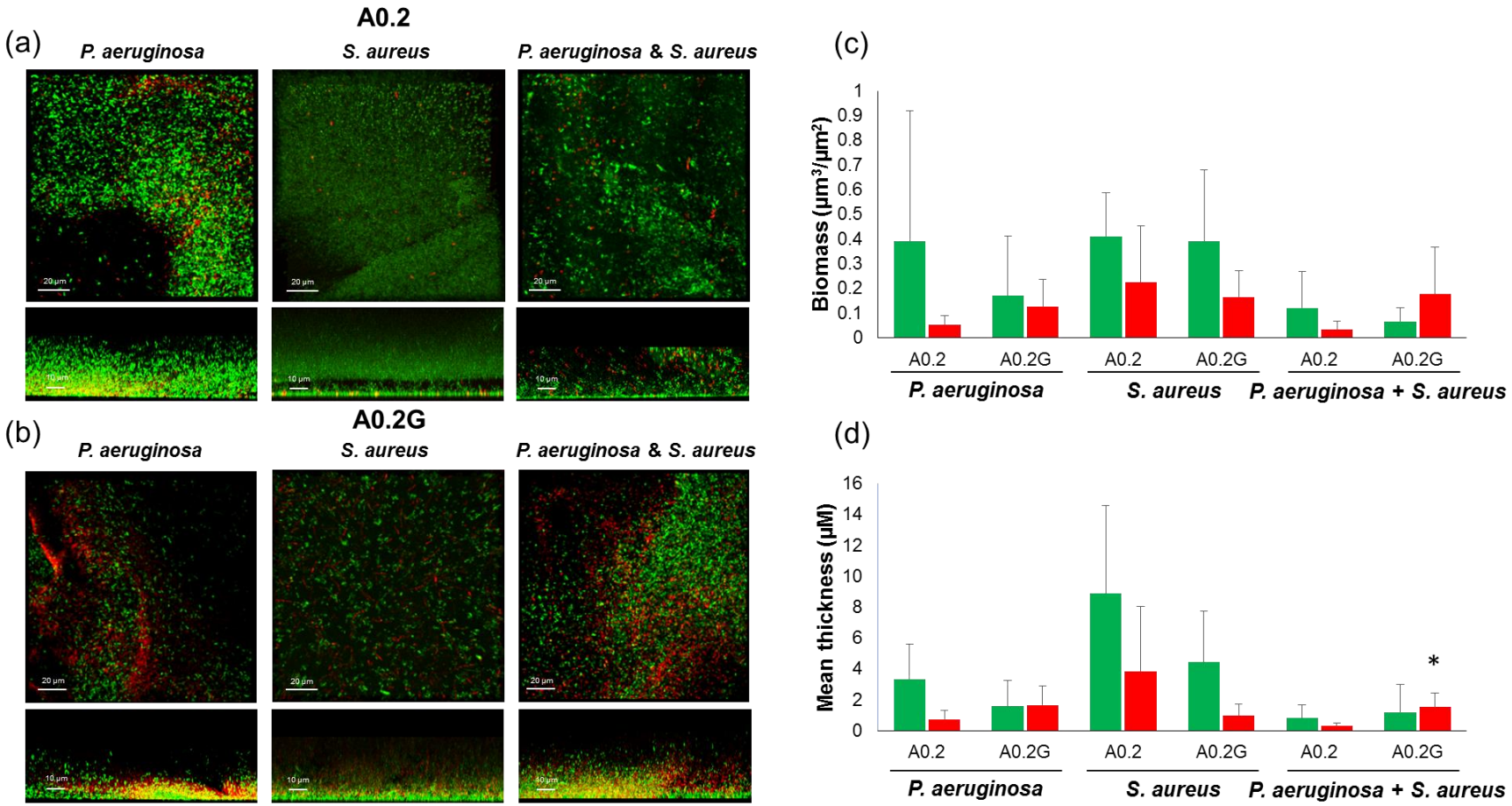

Figure 4. CLSM images of LIVE/DEAD® staining of 24 h single and dual species biofilms grown on CNF aerogels. (a) Control A0.2. (b) Oligo-bio-nanocomposite A0.2G. COMSTAT image analysis showing mean biofilm of LIVE (green) and DEAD (red) cells: (c) Biomass. (d) Thickness. (*significantly different compared to the equivalent no OligoG control; n=10 images each from n=3 replicates; $P<0.05$).

CLSM studies on the aerogel formulations revealed that untreated aerogels supported considerable biofilm biomass on the material surface (**Figure 4A**). Although a small number of dead cells were apparent in these images, non-vital bacterial cells within *P. aeruginosa* and mixed species biofilms increased on aerogels incorporating 2% OligoG (A0.2G; **Figure 4B,C**) however, this was not evident in the *S. aureus* biofilms. Whilst the OligoG aerogels (A0.2G) appeared to exhibit decreased bacterial biofilm biomass (**Figure 4C**) and thickness (**Figure 4D**), when compared to the untreated material (A0.2), these effects did not reach statistical significance (**Figure 4C,D** and **S2;** $P>0.05$). This lack of significance in the aerogel assays could be due to the inherent surface roughness of these materials, producing irregular biofilm structures, making them difficult to quantify.

Effect of the different CNF materials on production of the virulence factor pyocyanin by *P. aeruginosa* PAO1. The untreated CNF materials (A0.2 and F0.2) had no apparent effect on production of pyocyanin by PAO1 (**Figure 5**). However, incorporation of OligoG in both formulations (F0.2G, A0.2G) or PEG in the films (F0.2P) inhibited pyocyanin production ($P<0.05$). This inhibition was statistically significant in the F0.2P and A0.2G formulations.

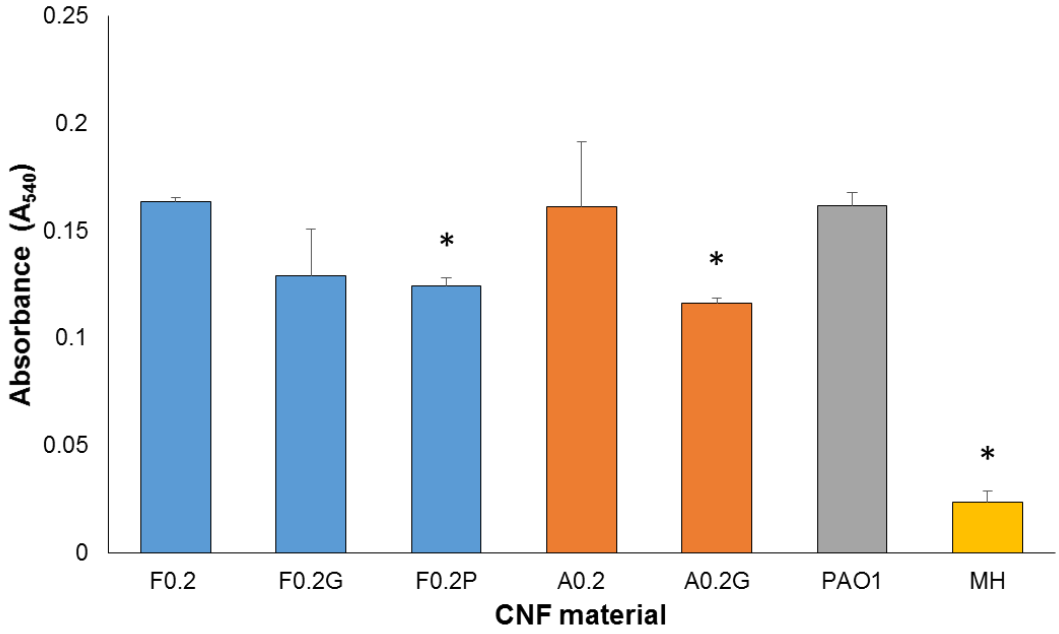

Figure 5. The effect of the different CNF formulations on pyocyanin production by *P. aeruginosa* PAO1. PAO1 and MH broth only were positive and negative controls respectively. (*significantly different compared to the PAO1 control; n=3; $P<0.05$).

SEM imaging of *P. aeruginosa* and *S. aureus* mixed species biofilms on CNF aerogels. Ion-milling of the aerogels (A0.2 and A0.2G) showed distinct differences between the 3-dimensional structure of the materials, with the CNF-OligoG bionanocomposite A0.2G displaying more numerous, tightly packed ruffles (stratification) in cross-section than the untreated aerogel A0.2 (**Figure 6A**). Biofilms were also clearly visible growing on the surface of the untreated formulation (A0.2), compared to the aerogel containing the antimicrobial alginate OligoG (A0.2G; **Figure 6B**).

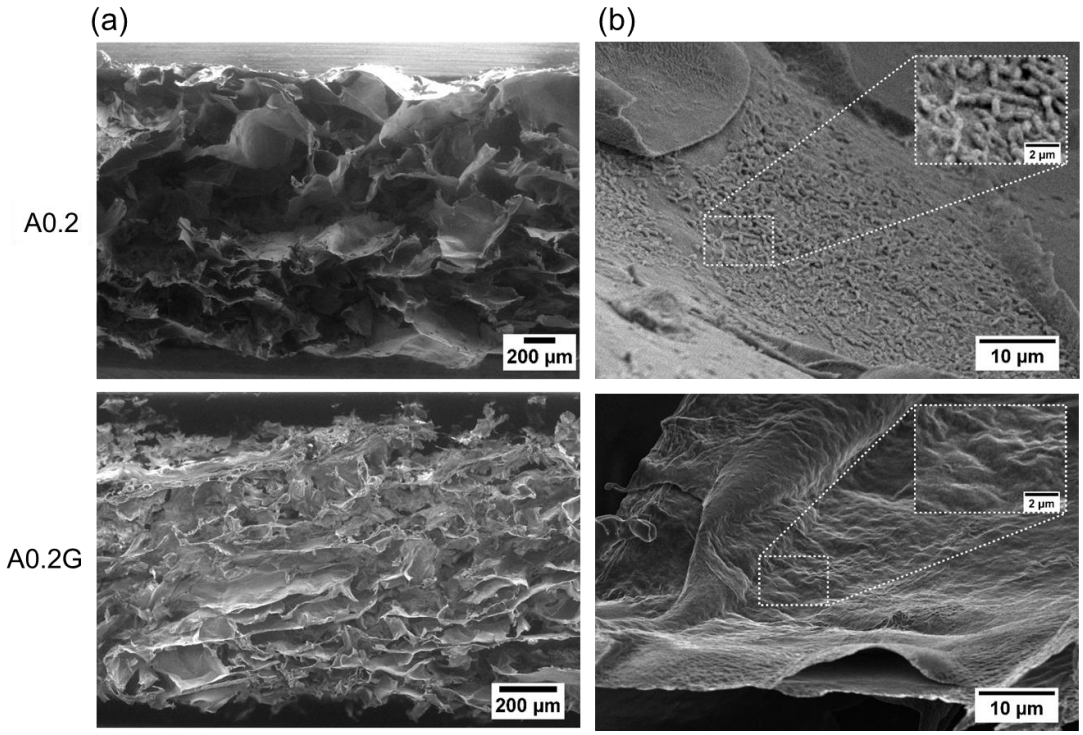

Figure 6. Scanning electron microscopy (SEM) imaging of a *P. aeruginosa* and *S. aureus* mixed species biofilm growing on untreated aerogels A0.2 or the OligoG bio-nanocomposite A0.2G. (a) Cross-sectional view following ion milling. (b) Aerial view with inset magnified areas showing biofilm growth.

DISCUSSION

Nanocellulose is increasingly being used for medical applications such as wound dressing materials, and as tissue engineering scaffolds to support host cell attachment and cell delivery.[33-35] Mechanically delaminated cellulose nanofibrils are attractive for biomedical applications due to their physical properties and biocompatibility.[36-38]

Importantly, alongside their sustainability, the recent ability to employ environmentally-friendly, non-toxic chemical processes, such as freeze-drying of aerogels as opposed to solvent exchange,[39] to produce CNF materials is environmentally attractive. Moreover, the surface chemistry of CNF materials can also be tailored (for example, by altering the choice of crosslinking ions such as calcium or copper) to have very different antimicrobial properties.[40] In the design of future CNF-based wound dressing materials, the incorporation of antimicrobials might clearly afford clinical benefit.

The incorporation of antimicrobials (e.g. silver or iodine) into wound dressing materials for sustained release has already been utilised in clinical settings. A recent study demonstrated that antibacterial agents can be readily released from freeze-dried CNF materials on conversion into a hydrogel in an aqueous environment,[41] highlighting the ability of stored dried aerogels to be 'activated' by hydration and still retain their antimicrobial properties, as might occur on exposure to an exudating wound. Importantly, we have previously reported the morphology and carboxyl content of CNF dressing materials obtained from the same *P. radiata* pulp fibers. The nanofibril width and carboxylic acid groups were quantified to be ~3.5 nm and ~0.9 mmol/g cellulose, respectively.[42,52] Here, we have used the low molecular weight antimicrobial OligoG in two formulations of CNF dressing materials, both as a surface-coating for films, and as a bionanocomposite by incorporation in the aerogels and shown retention of antimicrobial activity for both. Moreover, we demonstrated that these changes were associated with significantly decreased levels of pyocyanin production (an important virulence factor of *P. aeruginosa*) when OligoG was incorporated into the aerogel. We have previously shown that the CNF itself does not affect virulence factor production by *P.* aeruginosa,[11] so the effects seen in this study were the direct result of the antimicrobials used in the CNF formulations. In these experiments, film F0.2G appeared to have significantly greater antimicrobial efficacy than the aerogel formulation (A0.2G) in the mixed species biofilm model. Comparison of the effective release of OligoG from the films and aerogels has yet to be determined, but this may have played a role in the observed differences in antimicrobial efficacy.

Three-dimensional (3D) bioprinting allows the accurate deposition of specific biomaterials (including CNF) onto virtually any surface and shape.[42,43] Indeed, CNF-(high molecular weight) alginate bioinks are already being developed for cartilage regeneration.[44] The future use of OligoG as a constituent of a bioink; facilitating more

accurate surface deposition and "patterning" in tissue engineering applications such as dressing materials is immediately attractive. For such printing purposes, any bioinks used would need to be sufficiently liquid under shear to allow for micro-extrusion, regain viscosity after deposition to form 3D structures and have sufficient cross-linking abilities to maintain a 3D structure once printed;[45] all properties observed in sodium alginates.

In these experiments we also employed (as a control) polyethylene glycol (PEG), a widely employed, US Food and Drug Administration (FDA) approved, non-toxic, polymer that is frequently utilized in pharmaceutical preparations, including wound dressings.[46] PEG was used as it possesses inherent antibacterial properties and may be employed in the context of film formation as a plasticizer to increase flexibility.[29,47,48] In CNF films, the addition of PEG has been shown to effectively increase the maximum force and 'elongation strain at break' of CNF films, as well as their water absorption capacity.[48] Increasing the water absorption of films is potentially clinically useful for dressings for exudative wounds. Whilst the antibacterial effects of PEG have been described in the *in vitro* biofilm model here (which resembles/mimics the *in vivo* wound biofilm environment) incorporating PEG into the CNF materials did not result in any significant antimicrobial effects. Significantly reduced biofilm growth was only evident with the surface coated OligoG films.

Bionanocomposites are increasingly being developed for biomedical uses, such as wound dressing applications, in an attempt to utilise the beneficial and/or preferred chemical and physical properties of the individual constituents in a single biomaterial. Although to date, much of the research on nanocellulose composites appears to have focused on the use of bacterially-derived nanocellulose,[49-51] it has recently been demonstrated that TEMPO CNF gels, films and aerogels have a number of beneficial characteristics[10,11,19,29] and varying immunogenic properties, which could be valuable for specific wound healing applications.[52] In the present study, CNF aerogels containing OligoG, produced a material with considerably different physical characteristics (i.e. increased stratification) from the control materials and when compared to the air-dried films. Most importantly we have shown that OligoG, retains its' anti-bacterial and anti-biofilm properties in TEMPO CNF formulations.

CONCLUSIONS

This study showed that CNF-based nanomaterials, in film- or aerogel formulations, can be used to design and deliver sustainable dressing materials, with antibacterial and anti-biofilm properties and which are biodegradable in nature. The effectiveness of the alginate oligosaccharide OligoG as an antimicrobial agent against common wound pathogens in the "most difficult to treat" infection model (a bacterial biofilm system) was also apparent. Surface-coating (rather than a bionanocomposite material) proved the most effective against both single- and mixed-species bacterial biofilms, with the treated dressings exhibiting impaired bacterial growth, disrupted biofilm architecture and reduced bacterial virulence factor production *in vitro*. In addition to having a lower environmental impact than conventional polymer-based dressings, CNF-based nanomaterials have been shown here to have considerable potential clinical utility to deliver topical antibacterial and anti-biofilm wound healing therapies.

ASSOCIATED CONTENT

Supporting Information

Fig S1. Growth characteristics for *S. aureus* in CNF dispersions

Fig S2. COMSTAT image analysis of 24 h single and dual species biofilms

AUTHOR INFORMATION

Corresponding Authors

*E-mail: hillke1@cardiff.ac.uk. Tel.: +44 (0)2920 744252. Fax: +44 (0)2920 742442

*E-mail: gary.chinga.carrasco@rise-pfi.no. Tel.: +47 90836045. Fax: +47 73550999

ORCID

Katja E. Hill: 0000-0002-8590-0117

Gary.Chinga-Carrasco: 0000-0002-6183-2017

Notes

The authors (DWT and KEH) declare previous research funding from AlgiPharma AS.

ACKNOWLEDGEMENTS

This work was funded by the Research Council of Norway through the NANO2021 program, (Grant no. 219733) – NanoHeal: Bio-compatible cellulose nanostructures for

advanced wound healing applications. We thank AlgiPharma AS for providing the purified OligoG. We also thank Kate Powell, Lucy Sutton and Himanshu Kishnani for technical support and Andrew Thomas for γ-irradiation.

REFERENCES

(1) Abitbol, T.; Rivkin, A.; Cao, Y.; Nevo, Y.; Abraham, E.; Ben-Shalom, T.; Lapidot, S.; Shoseyov, O. Nanocellulose, a tiny fiber with huge applications. *Curr. Opin. Biotechnol.* **2016**, *39*, 76–88.

(2) Klemm, D.; Cranston, E. D.; Fischer, D.; Gama, M.;. Kedzior, S. A.; Kralisch, D.; Kramer, F.; Kondo, T.; Lindstrom, T.; Nietzsche, S.; Petzold-Welcke, K.; Rauchfuss, F. Nanocellulose as a natural source for groundbreaking applications in materials science: Today's state. *Mater. Today* **2018**, *21*, 720-748.

(3) Percival, S. L.; Hill, K. E.; Williams, D. W.; Hooper, S. J.; Thomas, D. W.; Costerton, J. W. A review of the scientific evidence for biofilms in wounds. *Wound Rep. Regen.* **2012**, *20*, 647–657.

(4) Hurlow, J.; Blanz, E.; Gaddy, J. A. Clinical investigation of biofilm in non-healing wounds by high resolution microscopy techniques. *J. Wound Care* **2016**, *25*, S11-S22.

(5) Ciofu, O.; Tolker-Nielsen, T.; Jensen, P. Ø.; Høiby, N. Antimicrobial resistance, respiratory tract infections and role of biofilms in lung infections in cystic fibrosis patients. *Adv. Drug Deliv. Rev*. **2015**, 85, 7–23.

(6) Davies, C. E.; Hill, K. E.; Wilson, M. J.; Stephens, P.; Hill, C. M.; Harding, K. G.; Thomas, D. W. Use of 16S ribosomal DNA PCR and denaturing gradient gel electrophoresis for analysis of the microfloras of healing and non-healing chronic venous leg ulcers. *J. Clin. Microbiol*. **2004**, *42*, 3549–3557.

(7) Davies, C. E.; Hill, K. E.; Stephens, P.; Wilson, M. J.; Harding, K. G.; Thomas, D. W. A prospective study of the microbiology of chronic venous leg ulcer tissue biopsies to reevaluate the clinical predictive value of tissue biopsies and swabs. *Wound Rep. Regen.* **2007**, *15*, 17-22.

(8) Loesche, M,: Gardner, S. E.; Kalan, L.; Horwinski, J.; Zheng, Q.; Hodkinson, B. P.; Tyldsley, A. S.; Franciscus, C. L.; Hillis, S. L.; Mehta, S.; Margolis, D. J.; Grice,

E. A. Temporal stability in chronic wound microbiota is associated with poor healing. *J. Invest. Dermatol*. **2017**, *137*, 237e244.

(9) Thomas S. 1997. A structured approach to the selection of dressings. *World Wide Wounds*, http://www.worldwidewounds.com/1997/july/Thomas-Guide/Dress-Select.html

(10) Powell, L. C.; Khan, S.; Chinga-Carrasco, G.; Wright, C. J.; Hill, K. E.; Thomas, D. W. An investigation of *Pseudomonas aeruginosa* biofilm growth on novel nanocellulose fiber dressings. *Carbohydr. Polym*. **2016**, *137*, 191–197.

(11) Jack, A. A.; Nordli, H. R.; Powell, L. C.; Powell, K. A.; Kishnani, H.; Johnsen, P. O.; Pukstad, B.; Thomas, D. W.; Chinga-Carrasco, G.; Hill K. E. The interaction of wood nanocellulose dressings and the wound pathogen *P. aeruginosa*. *Carbohydr. Polym*. **2017**, *157*, 1955-1962.

(12) Dufresne, A. Nanocellulose: a new ageless bionanomaterial. *Mater. Today* **2013**, *16*, 220-227.

(13) Isogai, A.; Saito, T.; Fukuzumi, H. TEMPO-oxidized cellulose nanofibers. *Nanoscale* **2011**, *3*, 71-85.

(14) Isogai, A. J. Wood nanocelluloses: fundamentals and applications as new bio-based nanomaterials. *Wood Sci.* **2013**, *59*, 449–459.

(15) Khalil, H. P. S. A.; Davoudpour, Y.; Islam M. N, Mustapha, A.; Sudesh, K.; Dungani, R.; Jawaid, M. Production and modification of nanofibrillated cellulose using various mechanical processes: A review. *Carbohydr. Polym*. **2014**, *99*, 649–665.

(16) Lasseuguette, E.; Roux, D.; Nishiyama, Y. Rheological properties of microfibrillar suspension of TEMPO-oxidized pulp. *Cellulose* **2008**, *15*, 425−433.

(17) Shinoda, R.; Saito, T.; Okita, Y.; Isogai, A. Relationship between length and degree of polymerization of TEMPO-oxidized cellulose nanofibrils. *Biomacromolecules* **2012**, *13*, 842−849.

(18) Chinga-Carrasco, G.; Syverud, K. Pretreatment-dependent surface chemistry of wood nanocellulose for pH-sensitive hydrogels. *J. Biomater. Appl.* **2014**, *29*, 423-432.

(19) Nordli, H. R.; Chinga-Carrasco, G.; Rokstad, A. M.; Pukstad, B. Producing ultrapure wood cellulose nanofibrils and evaluating the cytotoxicity using human skin cells. *Carbohydr. Polym*. **2016**, *150*, 65-73.

(20) Khan, S.; Tondervik, A.; Sletta, H.; Klinkenberg, G.; Emanuel, C.; Onsoyen, E.; Myrvold, R.; Howe, R. A.; Walsh, T. R.; Hill, K. E.; Thomas, D. W. Overcoming

drug resistance with alginate oligosaccharides able to potentiate the action of selected antibiotics. *Antimicrob. Ag. Chemother.* **2012**, *56***,** 5134-5141.

(21) Powell, L. C.; Sowedan, A.; Khan, S.; Wright, C. J.; Hawkins, K.; Onsoyen, E.; Myrvold, R.; Hill, K. E.; Thomas, D. W. The effect of alginate oligosaccharides on the mechanical properties of Gram-negative biofilms. *Biofouling* **2013**, *29*, 413-421.

(22) Powell, L. C.; Pritchard, M. F.; Emanuel, C.; Onsoyen, E.; Rye, P. D.; Wright, C. J.; Hill, K. E.; Thomas, D. W. A nanoscale characterization of the interaction of a novel alginate oligomer with the cell surface and motility of *Pseudomonas aeruginosa*. *Am. J. Respir. Cell Mol. Biol.* **2014**, *50*, 483-492.

(23) Pritchard, M. F.; Powell L. C.; Menzies, G. E.; Lewis, P. D.; Hawkins, K .; Wright C, Doull, I.; Walsh, T. R.; Onsøyen, E.; Dessen, A.; Myrvold, R.; Rye, P. D.; Myrset, A. H.; Stevens, H. N. E.; Hodges, L. A.; MacGregor, G.; Neilly, J. B.; Hill, K. E.; Thomas, D. W. A new class of safe oligosaccharide polymer therapy to modify the mucus barrier of chronic respiratory disease. *Mol. Pharma*. **2016**; *13*, 863-872.

(24) Pritchard, M. F.; Powell, L. C.; Khan, S.; Griffiths, P. C.; Mansour, O. T.; Schweins,R.; Beck, K.; Buurma, N. J.; Dempsey, C. E; Wright, C. J.; Rye, P. D.; Hill, K. E.; Thomas, D. W.; Ferguson E. L. The antimicrobial effects of the alginate oligomer OligoG CF-5/20 are independent of direct bacterial cell membrane disruption. *Sci. Rep.* **2017a**, *7*, 44731.

(25) Pritchard, M. F.; Powell, L. C.; Jack, A. A.; Powell, K.; Beck, K.; Florance, H.; Forton, J.; Rye, P. D.; Dessen, A.; Hill, K. E.; Thomas, D. W. A low molecular weight alginate oligosaccharide disrupts pseudomonal microcolony formation and enhances antibiotic effectiveness. *Antimicrob. Ag. Chemother*. **2017b**, *61*, e00762-17.

(26) Tøndervik, A.; Sletta, H.; Klinkenberg, G.; Emanuel, C.; Powell, L. C.; Pritchard, M. F.; Khan, S.; Craine, K. M.; Onsøyen, E.; Rye, P. D.; Wright, C.; Thomas, D. W.; Hill, K. E. Alginate oligosaccharides inhibit fungal cell growth and potentiate the activity of anti-fungals against *Candida* and *Aspergillus* spp. *Plos One*. **2014**, *9*, e112518.

(27) Pritchard, M. F.; Jack, A. A.; Powell, L. C.; Sadh, H.; Rye, P. D.; Hill, K. E.; Thomas, D. W. Alginate oligosaccharides modify hyphal infiltration of *Candida albicans* in an in vitro model of invasive human candidosis. *J. Appl. Microbiol.* **2017c**, *123***,** 625-636.

(28) Saito, T.; Nishiyama, Y.; Putaux, J. L.; Vignon, M.; Isogai, A. Homogeneous suspensions of individualized microfibrils from TEMPO-catalyzed oxidation of native cellulose. *Biomacromolecules* **2006**, *7*, 1687–1691.

(29) Sun, F.; Nordli, H. R.; Pukstad, B.; Gamstedt, E. K.; Chinga-Carrasco, G. Mechanical characteristics of nanocellulose-PEG bionanocomposite wound dressings in wet conditions. *J. Mech. Behav. Biomed. Mater*. **2017**, *69*, 377–384.

(30) Heydorn, A.; Nielsen, A. T.; Hentzer, M.; Sternberg, C.; Givskov, M.; Ersbøll, B. K.; Molin, S. Quantification of biofilm structures by the novel computer program COMSTAT. *Microbiology* **2000**, *146*, 2395–2407.

(31) Sarabhai, S.; Sharma, P.; Capalash, N. Ellagic acid derivatives from *terminalia chebula* Retz. downregulate the expression of quorum sensing genes to attenuate *Pseudomonas aeruginosa* PAO1 virulence. *PLoS One* **2013**, *8*, e53441.

(32) Chinga-Carrasco, G.; Averianova, N.; Kondalenko, O.; Garaeva, M.; Petrov, V.; Leinsvang, B.; Karlsen, T. The effect of residual fibres on the micro-topography of cellulose nanopaper. . *Micron* **2014**, *56*, 80–84.

(33) Lu, T.; Li, Q.; Chen, W.; Haipeng, Y. Composite aerogels based on dialdehyde nanocellulose and collagen for potential applications as wound dressing and tissue engineering scaffold. *Compos. Sci. Technol.* **2014**, *94*,132-138.

(34) Fernandes, E. M.; Pires, R. A.; Mano, J. F.; Reis, R. L. Bionanocomposites from lignocellulosic resources: Properties, applications and future trends for their use in the biomedical field. *Prog. Polym. Sci*. **2013**, *38*, 1415-1441.

(35) Fu, L. N.; Zhou, P.; Zhang, S. M.; Yang, G. Present status and applications of bacterial cellulose-based materials for skin tissue repair. *Carbohydr. Polym*. **2013**, *92*, 1432-1442.

(36) Syverud, K.; Pettersen, S. R.; Draget,K.; Chinga-Carrasco, G. Controlling the elastic modulus of cellulose nanofibril hydrogels – scaffolds with potential in tissue engineering. *Cellulose* **2015**, *22*, 473–481.

(37) Lou, Y. R.; Kanninen, L.; Kuisma, T.; Niklander, J.; Noon, L. A.; Burks, D.; Urtti, A.; Yliperttula, M. The use of nanofibrillar cellulose hydrogel as a flexible three-dimensional model to culture human pluripotent stem cells. *Stem Cells Dev.* **2014**, *23*, 380–392

(38) Ninan, N.; Muthiah, M.; Park, I.-K.; Elain, A.; Thomas, S.; Grohens, Y. Pectin/carboxymethyl cellulose/microfibrillated cellulose composite scaffolds for tissue engineering. *Carbohydr. Polym*. **2013**, *98*, 877–885.

(39) Oksman, K.; Aitomäki, Y.; Mathew, A. P.; Siqueira, G.; Zhou, Q.; Butylina, S.; Tanpichai, S.; Zhou, X.; Hooshmand, S. Review of the recent developments in cellulose nanocomposite processing. *Compos. Pt. A-Appl. Sci. Manuf.* **2016**, *83*, 2–18.

(40) Basu, A.; Heitz, K.; Strømme, M.; Welch, K.; Ferraz N. Ion-crosslinked wood-derived nanocellulose hydrogels with tunable antibacterial properties: Candidate materials for advanced wound care applications. *Carbohydr. Polym.* **2018**, *181*, 345–350.

(41) Paukkonen, H.; Kunnari, M.; Laurén, P.; Hakkarainen, T.; Auvinen, V-V.; Oksanen, T.; Koivuniemi, R.; Yliperttula, M.; Laaksonen, T. Nanofibrillar cellulose hydrogels and reconstructed hydrogels as matrices for controlled drug release. *Int. J. Pharma.* **2017**, *532*, 269–280.

(42) Rees, A.; Powell, L. C.; Chinga-Carrasco, G.; Gethin, D. T.; Syverud, K.; Hill, K. E.; Thomas, D. W. 3D Bioprinting of carboxymethylated-periodate oxidized nanocellulose constructs for wound dressing applications. *BioMed Res. Int.* **2015**, 925757.

(43) Chinga-Carrasco, G. Potential and limitations of nanocelluloses as components in biocomposite inks for three-dimensional bioprinting and for biomedical devices. *Biomacromolecules*. **2018** *19*, 701-711.

(44) Markstedt, K.; Mantas, A.; Tournier, I.; Martínez Ávila, H.; Hägg, D.; Gatenholm, P. 3D bioprinting human chondrocytes with nanocellulose−alginate bioink for cartilage tissue engineering applications. *Biomacromolecules* **2015**, *16*, 1489−1496.

(45) Aljohani, W.; Ullah, M. W.; Zhang, X.; Yang, G. Bioprinting and its applications in tissue engineering and regenerative medicine. *Int. J. Biol. Macromol.* **2018**, *107*, 261–275.

(46) Chen, S-L,; Fu, R-H,; Liao, S-F,; Liu, S-P,; Lin, S-Z,; Wang, Y-C. A PEG-based hydrogel for effective wound care management. *Cell Transplant.* **2018**, *27*, 275–284.

(47) Chirife, J.; Herszage, L.; Joseph, A.; Bozzini, J. P.; Leardini, N.; Kohn, E. S. *In vitro* antibacterial activity of concentrated polyethylene glycol 400 solutions. *Antimicrob. Agents Chemother.* **1983**, *24*, 409-412.

(48) Tehrani, Z., Nordli, H.R., Pukstad, B., Gethin, D.T., Chinga-Carrasco, G. Translucent and ductile nanocellulose-PEG bionanocomposites – a novel substrate with potential to be functionalized by printing for wound dressing applications. *Ind. Crop. Prod.* **2016**, *93*, 193–202.

(49) Zmejkoski, D.; Spasojevic, D.; Orlovska, I.; Kozyrovska, N.; Sokovic, M.; Glamoclija, J.; Dmitrovic, S.; Matovic, B.;Tasic, N.; Maksimovic, V.; Sosnin, M.; Radotic, K. Bacterial cellulose-lignin composite hydrogel as a promising agent in chronic wound healing. *Int. J. Biol. Macromol.* **2018,** *118*, 494-503.

(50) Gatenholm, P.; Klemm, D. Bacterial nanocellulose as a renewable material for biomedical applications. *MRS Bull*. **2010**, *35*, 208-213.

(51) Grande, C. J.; Torres, F. G.; Gomez, C. M.; Bano, M. C. Nanocomposites of bacterial cellulose/hydroxyapatite for biomedical applications. *Acta Biomater*. **2009**, *5*, 1605-1615.

(52) Nordli, H. R.; Pukstad, B.; Chinga-Carrasco, G.; Rokstad, A. M. Ultrapure wood nanocellulose – assessments of coagulation and initial inflammation potential. *ACS Appl. Bio Mater*. **2019**, *2*, 1107−1118.